Single particle transport through carbon nanotube wires: Effect of defects and polyhedral cap

M. P. Anantram and T. R. Govindan

NASA Ames Research Center, M/S T27A-1, Moffett Field, CA 94035-1000, U. S. A.

1 Introduction

The ability to manipulate carbon nanotubes with increasing precision has enabled a large number of successful electron transport experiments. These studies have primarily focussed on characterizing transport through both metallic and semiconducting wires [1, 2, 3, 4, 5, 6]. Reference [1] demonstrated ballistic transport in single-wall nanotubes for the first time, although the experimental configuration incurred large contact resistance. Subsequently, methods of producing low contact resistances have been developed and two terminal conductances smaller than 50kΩ have been repeatably demonstrated in single-wall and multi-wall nanotubes. In multi-wall nanotubes, reference [5] demonstrated a resistance of approximately $h/2e^2$ in a configuration where the outermost layer made contact to a liquid metal. This was followed by the work of reference [6] where a resistance of $h/27e^2$ (approximately 478Ω) was measured in a configuration where electrical contact was made to many layers of a multi-wall nanotube. References [5] and [6] note that each conducting layer contributes a conductance of only $2e^2/h$, instead of the $4e^2/h$ that a single particle mode counting picture yields. These small resistances have been obtained in microns long nanotubes, making them the best conducting molecular wires to date. The large conductance of nanotube wires stems from the fact that the crossing bands of nanotubes are robust to defect scattering [7, 8, 9].

Transport details through CNT caps is important for many purposes. In STM experiments, electrons tunnel from the substrate being probed to the tip of a capped or open nanotube. Experiments in molecular electronics may also use a nanotube tethered to metal or other parts of the circuit. For these applications, understanding the physics of electron transport through capped nanotubes is relevant. To gain this understanding, references [10, 11, 12, 13] analyzed the wave function and density of states of capped nanotubes, and reference [14] recently studied the electron transmission probability through polyhedral capped nanotubes.

In the present work, we extend previous work [14] to include the effects of an arbitrary number of leads to the nanotube. We also examine the role of defects in determining nanotube conductance. In section 2 we discuss a method to calculate the transmission through nanotubes with an arbitrary number of leads. In section 3, we review the role of defects in determining the conductance of nanotubes at band-

center energies [7, 8, 9] and at higher energies [9]. The discussion of the role of defects closely follows our earlier work in reference [9]. Two types of defects are discussed here. The first is weak uniform disorder and the second is strong isolated defects. The transmission of electrons at the band center is reasonably insensitive to the first type of defect but is greatly diminished by the second. Transmission through caps is discussed in section 4, and this discussion closely follows our earlier work in reference [14]. Our discussion is for polyhedral caps. The transmission is found to correspond to the local density of states (LDOS) at all energies except those corresponding to the localized states. Hybridization between substrate and carbon nanotube states leads to interference paths that yield strong transmission antiresonances. The presence of defects in the nanotube can transform these antiresonances to resonances. The current carrying capacity of these resonances, however, depends on the location of the defects. Conclusions of our study are presented in section 5.

2 Method

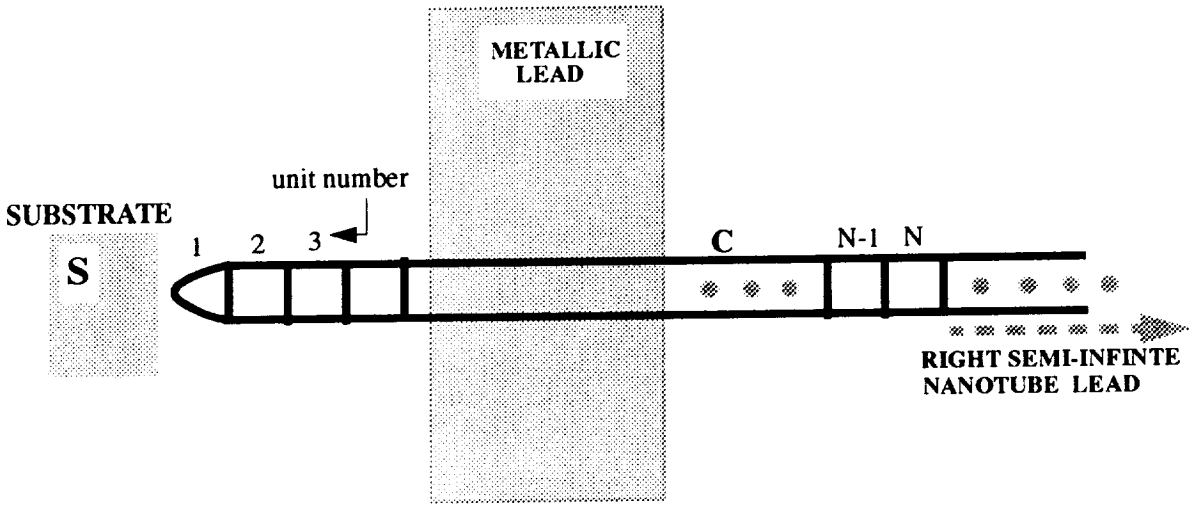

Figure 1: Carbon nanotube in contact with three leads: a semi-infinite carbon nanotube on the right, and metallic leads in the center and in close proximity to the cap at the left.

In this section, we present the model and method used to analyze transport through CNT. Fig1. shows a nanotube (denoted by C) with three leads, a semi-infinite carbon nanotube on the right, a metallic lead in the center and a substrate (denoted by S) which is the metallic lead in close proximity to the cap at the left. Placing the metallic lead at the center of the nanotube is akin to the experiments in reference [1], where the metal is side-contacted to the nanotube. The transmission and LDOS are calculated from the Green's function of the nanotube connected to the leads. The leads are by definition objects that are capable of injecting electrons into the device, and so are typically modeled as either metals [15] or semi-infinite carbon nanotubes. The Green's function is calculated by the procedure given in references [16, 17] and [18]. The equation governing the Green's function is:

$$\left[EI - H_C - \sum_{\alpha} \Sigma_{\alpha}^{r}\right] G_C^r(E) = I, \tag{1}$$

where H_C is the Hamiltonian of the isolated nanotube and I is the identity matrix of size equal to the number of atoms in C [17]. Σ_{α}^{r} is the retarded self energy arising due

to connection with lead α, and is given by,

$$\Sigma_\alpha^r(E) = V_{C-\alpha} g_\alpha^r(E) V_{\alpha-C} \ . \tag{2}$$

$V_{C-\alpha}$ ($V_{\alpha-C}$) is the Hamiltonian representing the interaction between C (lead α) and lead α (C), and g_α^r is the Green's function of the isolated lead. Σ_α^r is a square matrices of size equal to the number of atoms in C. Note that only sub-matrices of Σ_α^r that correspond to atoms in C coupled to lead α are non-zero. Further, only those elements of g_α^r that couple atoms (nodes) in α to C are required. The real part of the diagonal components of Σ_α^r represents the change in on-site potential of the C atoms, and the imaginary part is responsible for injection of electrons from α to C. In general, the off-diagonal elements of Σ_α^r cannot be neglected, since they play an important role in determining transport characteristics.

The single particle LDOS at site i [$N_i(E)$] and transmission probability between leads α and β [$T_{\alpha\beta}(E)$] at energy E are obtained by solving Eq. (1) for the diagonal element G_{ii}^r and the off-diagonal sub-matrix of G^r in C that couple α and β [17, 18]:

$$N_i(E) = -\frac{1}{\pi} Im[G_{ii}^r(E)] \tag{3}$$

$$T_{\alpha\beta}(E) = Trace[\Gamma_\alpha G^r \Gamma_\beta G^a] \ . \tag{4}$$

$\Gamma_\alpha = 2\pi V_{C-\alpha} Im[g_\alpha^r(E)] V_{\alpha-C}$, where Im extracts the imaginary part.

For computational efficiency and to calculate the transmission through a long nanotube region, we divide the structure C into N smaller units with each unit typically representing a few rings of atoms along the circumference of the tube (Fig. 1). The units need not necessarily be of the same size, but the main idea is to order atoms in the units such that $[EI - H_C - \sum_\alpha \Sigma_\alpha^r]$ is a tridiagonal block matrix,

$$\begin{pmatrix} A_1 & B_{12} & O & O & O & O & O \\ B_{21} & A_2 & B_{23} & O & O & O & O \\ O & B_{32} & \bullet & \bullet & O & O & O \\ O & O & \bullet & \bullet & \bullet & O & O \\ O & O & O & \bullet & \bullet & \bullet & O \\ O & O & O & O & \bullet & \bullet & B_{N-1,N} \\ O & O & O & O & O & B_{N,N-1} & A_N \end{pmatrix} \begin{pmatrix} G_{11}^r \\ G_{21}^r \\ \bullet \\ \bullet \\ \bullet \\ G_{N-11}^r \\ G_{N1} \end{pmatrix} = \begin{pmatrix} 1 \\ O \\ \bullet \\ \bullet \\ \bullet \\ O \\ O \end{pmatrix} . \tag{5}$$

The advantage of casting the matrix in the block tridiagonal form is the efficiency of matrix inversion compared to a non-tridiagonal sparse matrix [19]. If the ith unit contains N_i atoms, then the diagonal block, $A_i = [EI - H_C - \sum_\alpha \Sigma_\alpha^r]_{ith\ block}$ is a N_i by N_i square matrix. The off diagonal sub-matrix B_{ij} represents coupling between units i and j, and is a N_i by N_j rectangular matrix, where N_j is the number of atoms in unit j. Also, note that B_{ij} is non zero only when $|i-j| = 1$. In Eq. (4), computing $T_{\alpha\beta}$ only requires solving for the off-diagonal rectangular matrix $G_{i_\alpha i_\beta}$ between units i_α and i_β. i_α and i_β are units representing carbon atoms connected to leads α and β respectively.

Finally, the single-particle Hamiltonian of the nanotube is [20],

$$H_C = \sum_i \epsilon_i c_i^\dagger c_i + \sum_{i,j} \left[t_{ij} c_i^\dagger c_j + c.c \right] \ , \tag{6}$$

where, ϵ_i is the on-site potential and t_{ij} is the hopping parameter between lattice sites i and j. $\{c_i^\dagger,\ c_i\}$ are the creation and annihilation operators at site i. The Hamiltonian between a nanotube (C) and metal (M) is,

$$H_{CM} = \sum_{i \in C, r \in M} \left[\tau_{ir} c_i^\dagger d_r + c.c \right] \ , \tag{7}$$

where, τ_{ix} is the hopping parameter between lattice sites i of the nanotube and x of the metal. $\{d_x^\dagger,\ d_x\}$ are the creation and annihilation operators at site x in the metal. The Hamiltonian of the metal is similar to Eq. 6, except that the on-site potential, hopping parameters and lattice coordination corresponds to that of the metal.

3 Defects

Having described the system, model and method, we now consider the effect of two types of defects on transport. The effect of weak uniform disorder on the localization length of nanotubes was first considered in reference [7], within the context of a two band model by calculating the elastic mean free path and relating the mean free path to the localization length. Reference [9] independently calculated the transmission probability through disordered nanotubes of varying lengths connected to disorder free semi-infinite carbon nanotube leads. Weak uniform disorder is herein modeled by randomly changing the on-site potential of the atoms, $\epsilon_i \rightarrow \epsilon_i + \delta\epsilon_i$ in Eq. (6), where $\delta\epsilon_i$ is randomly chosen from the interval $\pm|\epsilon_{random}|$ at all lattice points. A larger $|\epsilon_{random}|$ implies larger disorder.

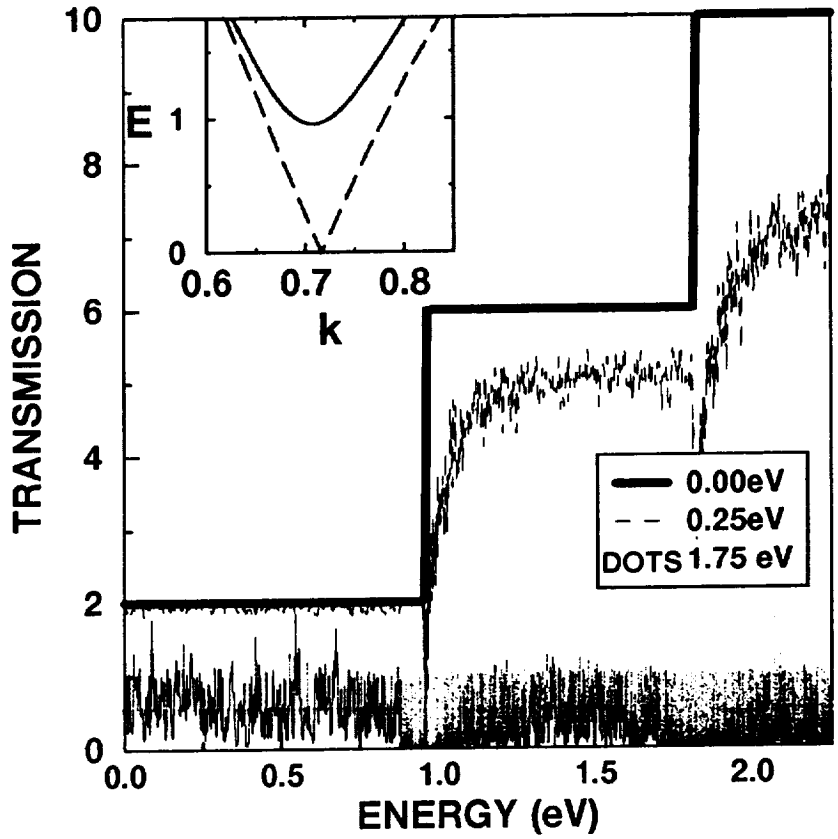

Figure 2: Transmission probability versus energy of a (10,10) nanotube with disorder distributed over a length of 1000 Å. *The significant features here are the robustness of the transmission probability around the zero of energy as the strength of disorder is increased and the dip in transmission probability at energies close to the beginning of the second sub-band.* The inset shows energy versus wave vector for the first (solid) and the second sub-band (dashed); the velocity of electrons at the minima of the solid line is zero. (From reference [9].)

Fig. 2 is a plot of the transmission probability versus energy for three different values of disorder. There are three main points that we want to convey here. The first is the insensitivity of the transmission probability to disorder at energies close to

the band center, where only two sub-bands are present. $|\epsilon_{random}| = 0.25eV$ results in an insignificant reflection probability. A large value of $|\epsilon_{random}| = 1.75eV$ causes more reflection but insufficient to change the transmission drastically at the band center. The reason for this robustness is that electrons in a CNT can find transmission paths around defects because of the large number of atoms in a cross section. And, importantly they result in only two modes at the band center into which electrons can reflect. If this intuitive explanation is correct, we would expect that for a given $|\epsilon_{random}|$, the transmission should depend on the radius of the tube. That is, with increasing number of atoms along the circumference of the tube, the transmission should increase. In Fig. 3, we show that this is indeed the case by comparing the transmission of (10,10), (5,5) and (12,0)-zigzag tubes, each with a 1000 $\AA$ disordered region. The diameters of these tubes are 13.4 $\AA$, 9.4 $\AA$ and 6.7 $\AA$ respectively. For the (10,10) and (5,5) tubes, the band structure at energies close to the Fermi energy are similar [20]. However, the number of atoms in a unit cell of a (5,5) tube is only half of that of a (10,10) tube (20 and 40 atoms, respectively). The important point here is that although the transmission of disorder-free (10,10) and (5,5) tubes at energies around the band center are identical, transmission is smaller for the (5,5) tube in the presence of disorder. The (12,0) zigzag tube has a diameter between that of the (10,10) and (5,5) tubes. Correspondingly, the average transmission is between the values of the (10,10) and (5,5) tubes. Reference [8], using analytical expressions addresses the reason for small reflection at the band center.

The second point we wish to make about Fig. 2 concerns localization. We have calculated conductance as a function of the length of the disordered region. For disordered regions larger than the localization length (L_0), the conductance of any quasi one dimensional structure has been predicted to decrease exponentially with length, $g = g_0\ exp(-L/L_0)$, in the phase coherent limit [21]. For lengths shorter than the localization length, the decrease in conductance is not given by this relation. We observe this to be the case in Fig. 4. The inset of Fig. 4 shows that the conductance does change exponentially with length for disordered regions larger than L_0. The value of L_0 corresponding to disorder strengths of 1eV and 1.75eV are 3353 $\AA$ and 1383 $\AA$ respectively. We note that in Fig. 4 the conductance of a micron long (10,10) nanotube with $|\epsilon_{random}| = 0.25eV$ is *large*, approximately $1.5\frac{e^2}{h}$.

The third point we want to convey is the large decrease in transmission probability at energies where many sub-bands are present, and especially the dip in transmission probability corresponding to the opening of a new sub-band. The origin of this dip in transmission probability is the low velocity electrons in the second sub-band (inset of Fig. 2) and can be explained as follows. In a perfect lattice, the velocity (dE/dk) of electrons in the second sub-band and with an energy close to the minimum is nearly zero. These low-velocity electrons are easily reflected by the smallest of disorders. Disorder causes mixing of the first and second sub-bands. As a result, electrons incident in either sub-band at these energies have a large reflection coefficient (in comparison to electrons with energies close to the band center). Increasing the disorder strength results in further reduction of the conductance and also results in the broadening of the dip. A dip in transmission probability at the formation of new sub-bands was also found in in reference [22], in their study of quasi one dimensional wires. At energies away from the band center, many sub-bands exist. As a result, an electron incident at these energies has many sub-bands into which it can reflect. This accompanied by the large reflection due to low velocity states at sub-band openings leads to a transmission probability that is greatly diminshed in comparison to that at low energies, where there are only two sub-bands (Fig. 2). For example, in Fig. 2, the transmission probability

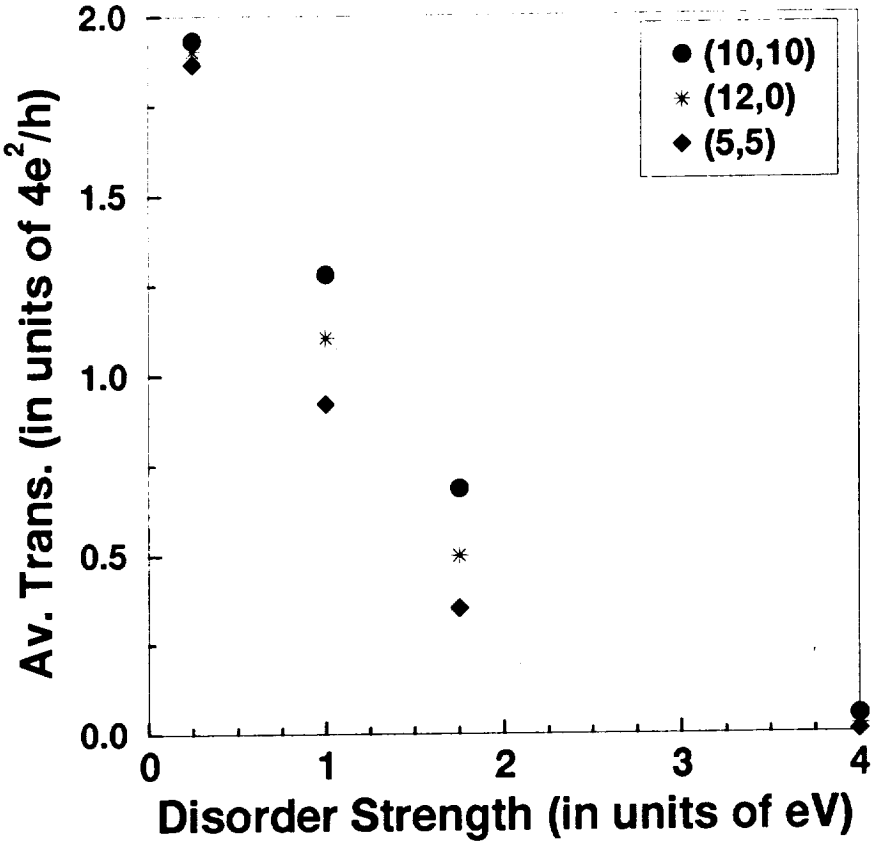

Figure 3: Average transmission probability at the band center versus disorder strength for wires of different diameter. The transmission probability has been averaged over a thousand different realizations of the disorder. The main feature here is that the average transmission probability decreases with decrease in the number of atoms along the circumference of the wire. (From reference [9].)

at $E = 2eV$ is equal to 10 in a disorder-free (10,10) nanotube, while even a small $|\epsilon_{random}| = 0.25eV$ reduces this to a about 6 or 7.

Although transmission through CNTs is relatively insensitive to weak-disorder type defects, there may be other type of defects that are capable of changing the transmission probability more dramatically at the band center. We consider one such defect type below.

Strong isolated defects (defined to be lattice locations onto which an electron cannot hop) are isolated due to a either a large mismatch in the on-site potential or weak bonds with neighbors. It was shown in reference [23] that scattering from a single such defect causes a maximum reduction in the transmission probability at the band center E=0. The transmission probability of a 1000 $\AA$ long (10,10) nanotube with ten defects scattered randomly along the length is plotted in Fig. 5. The main point is that independent of the exact location of these defects, a *transmission gap* opens at the center of the band as the number of defects is increased. The width of the transmission gap increases with the increase in defect density [9]. The transmission probability also decreases sharply at energies corresponding to the opening of the second sub-band, although this effect is weak compared to that due to weak uniform disorder. While there is as yet no experimental evidence for such strong scattering, we expect that when the Fermi energy is close to $E = 0$, the low bias conductance will be small in the presence of such defects [9].

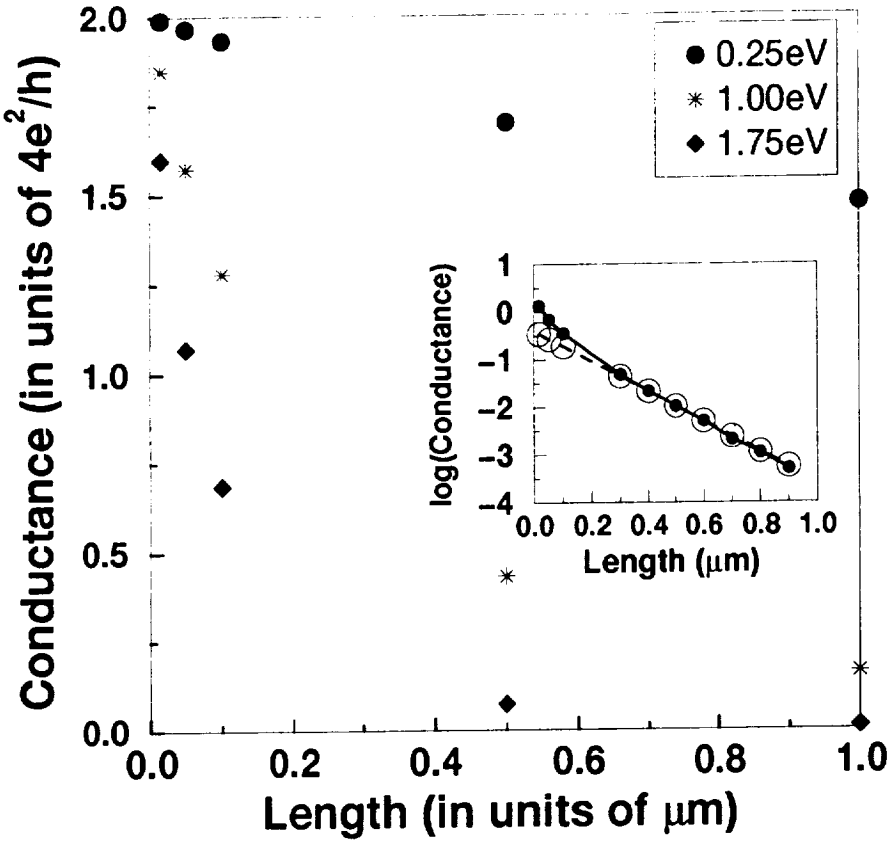

Figure 4: Conductance versus length of the (10,10) CNT. While for the large disorder strengths, the conductance is significantly affected by disorder, the conductance is reasonably large for the smaller values of disorder. *This demonstrates the robustness of these wires to weak uniform disorder at energies close to the band center.* Inset: log(Conductance) versus length for disorder strength of 1.75eV, in a (5,5) CNT. The solid line/filled circle corresponds to the simulation and the dashed line/empty circle corresponds to that obtained using $g = g_0 exp(-L/L_0)$. (From reference [9].)

4 Transport through a polyhedral cap

The discussion of transport through capped nanotubes is restricted to armchair tubes with polyhedral caps. The discussion closely follows our work in reference [14]. The main issues we address here are: (i) the relationship between the LDOS and the transmission probability through cap atoms in a defect free CNT, (ii) the effect of the localized discrete energy levels in the cap, and (iii) the effect of defects on tunnel current/transmission.

The transmission probability and LDOS are calculated for a (10,10) nanotube with a polyhedral cap (Fig. 6). This cap has a five-fold symmetry, with one pentagon at the cap center and five pentagons placed symmetrically around it. The geometry is the same as in Fig. 1 but with the metal contact at the center absent. The transmission probability is calculated from the substrate to the semi-infinite nanotube lead at the right hand side of Fig. 1 (without the metal contact at the center). We assume only a single atom in the cap makes contact with the substrate. The atom making contact is shown circled in Fig. 6. The contact is modeled by an energy independent self-energy [in Eqs. (1) and (2)], Σ_S^r. Within the context of a single parameter tight binding Hamiltonian, the polyhedral cap has localized states (with an infinite life-time) that decay into the nanotube [10]. Coupling of the cap to the substrate causes hybridization between the substrate states, nanotube continuum states and localized states of the polyhedral cap. This hybridization transforms the localized states into quasi-localized

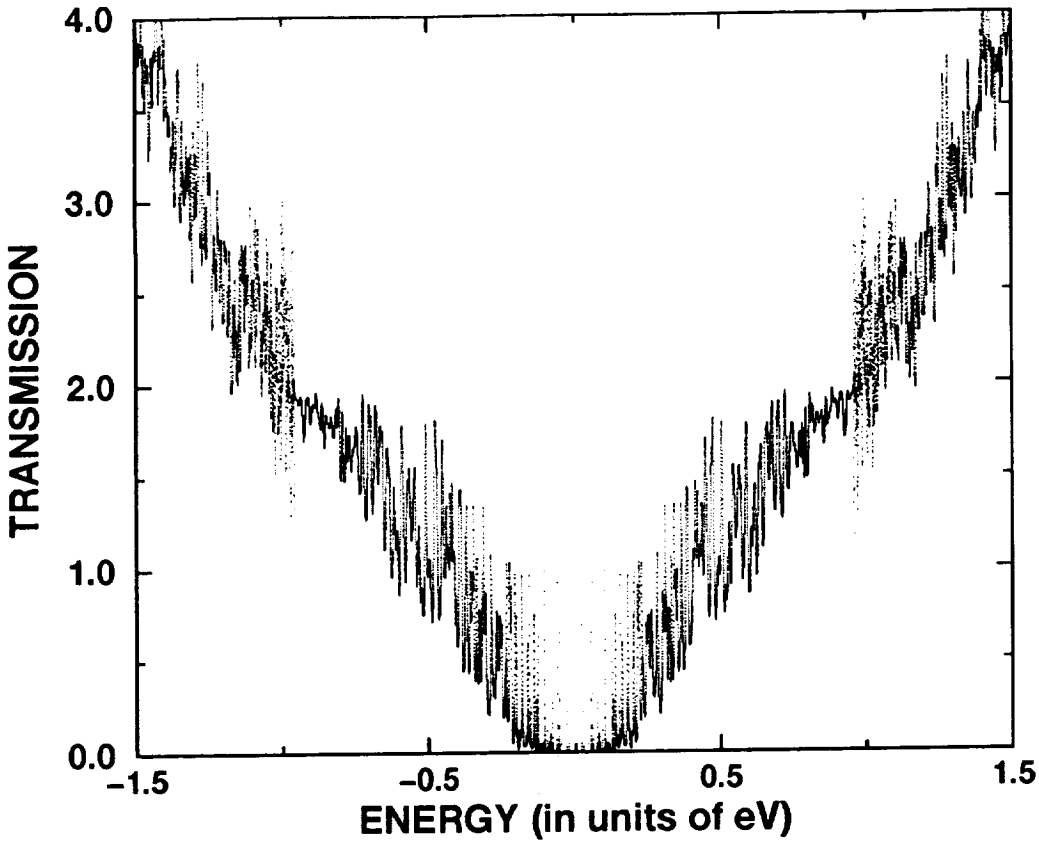

Figure 5: Transmission probability versus energy of a (10,10) CNT with ten strong isolated scatterers sprinkled randomly along a length of 1000 Å. The main prediction here is the opening of a gap in the transmission probability around the zero of energy. The transmission probability of a defect-free tube is shown in Fig. 2. (From reference [9].)

states (finite life-time).

The density of states averaged over the cap and over unit cells at various distances away from the cap is shown in Fig. 7. The distance is measured in terms of the number of unit cell lengths of the (10,10) nanotube. In Fig. 7, there are two localized states in the energy range considered, one around 0.25 eV and the other around -1.5 eV. The transmission probability (Fig. 8) corresponds directly to the LDOS at most energies. The major difference is near the localized state energy, where *the LDOS peaks corresponds to transmission zeroes.* The solid line in Fig. 8 is for $\Sigma_S^r = i \cdot 0.25\text{eV}$, a purely imaginary number, which corresponds to a smooth antiresonance. However, when the cap makes contact to the substrate Σ_S^r would in general also have a real part. The dashed curve in Fig. 8 corresponds to $\Sigma_S^r = 0.25 + i \cdot 0.25\text{eV}$. This curve retains the anti-resonance feature, but the shape has changed as a result of the non zero real part, which is consistent with earlier calculations in quantum wires with stubs [24]. The transmission dip arises from hybridization of localized and continuum states via coupling to the substrate, in a manner akin to Fano resonances [25]. States in the CNT cap comprise localized (ϕ_L) and continuum (ϕ_C) states that are uncoupled to each other. Bringing the substrate in close proximity to the cap couples ϕ_L and ϕ_C to the substrate states (ϕ_S). As a result, electrons can be transmitted from ϕ_S to ϕ_C either directly ($\phi_S \rightarrow \phi_C$), through the localized states ($\phi_S \rightarrow \phi_L \rightarrow \phi_S \rightarrow \phi_C$), and through higher order interactions. The interference between these paths gives rise to the transmission antiresonances.

We now consider changes to the antiresonance picture due to defects in a tube. A

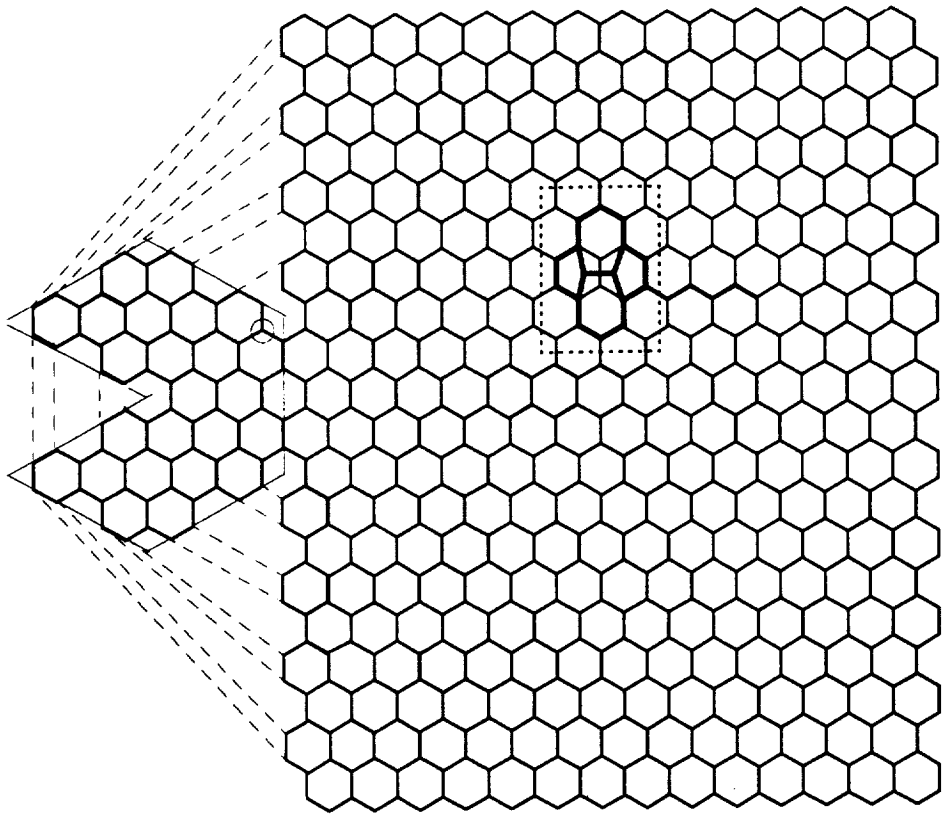

Figure 6: (10,10) carbon nanotube with a polyhedral cap. The dashed lines connect equivalent sites of the cap and nanotube in this two dimensional representation. The dashed box shows a bond rotation defect (From reference [14].)

defect locally mediates mixing/hybridization of localized and continuum states. This leads to transmission paths similar to a double barrier resonant tunneling structure, where the two scattering centers provide coupling between the substrate, the nanotube localized state and the defect. In addition, the paths leading to the transmission antiresonance discussed previously also exist, and are accounted in the model.

To demonstrate the effects of defects on transmission through a polyhedral cap, we consider a topological bond rotation defect (box in Fig. 6) [26]. The LDOS remains similar to Fig. 7 but in comparison to Fig. 8, the transmission probability has changed significantly around the localized energy levels as shown in Fig. 9. Resonant peaks appear in the transmission probability. The resonance width here is determined by two contributions: hybridization of the localized and continuum cap states due to the substrate and the distance of defect from the cap. In particular, the second contribution depends on $| < \phi_C | H_{defect} | \phi_L > |$, where H_{defect} is Hamiltonian of the defect. $|\phi_L|^2$ (or the density of states of the localized state) decays with distance away from the cap. As a result, the width of the transmission resonance depends on location of the defect. Fig. 9 shows the transmission for two different distances of the defect from the cap (L_D): $L_D = 7$ and $L_D = 15$, where L_D is in units of the one dimensional unit cell length of armchair tubes. The main feature in Fig. 9 is that the *transmission resonance width becomes smaller as distance of the defect from the cap increases.* This can be understood from the fact that the strength of hybridization between continuum and localized states in the cap caused by the defect ($| < \phi_C | H_{defect} | \phi_L > |$) decreases as distance of the defect increases from the cap. In terms of the current carrying capacity, clearly from Fig. 9, the resonant state is capable of carrying a large current per unit

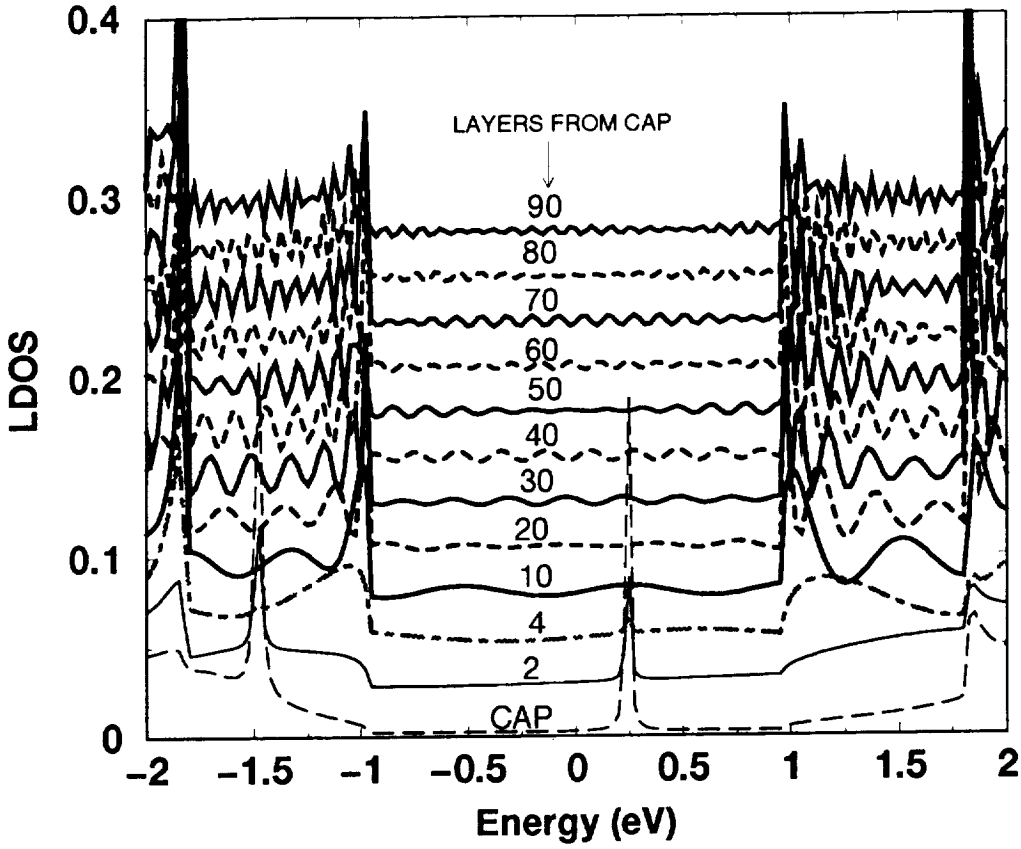

Figure 7: The bottom-most curve is the DOS averaged over all atoms in the cap. The quasi-localized level is strongly peaked. Other curves represent the DOS averaged over a unit cell of the armchair tube at varying distances from the cap. The curves have been displaced by multiples of 0.025 along the y-axis. The circled site in Fig. 6 makes contact to the substrate with coupling strength $\Sigma_S^r = i \cdot 0.25eV$

energy compared to that of the background energies.[a]

5 Conclusions

Two aspects of single particle transport through carbon nanotube wires were reviewed. In section 3, calculations of the transmission probability through carbon nanotube wires with simple defect models were discussed [9]. *It was shown that carbon nanotube wires with weak uniform disorder are relatively insensitive to back scattering at energies where only the crossing bands (close to E=0) contribute to transport.* The localization length of nanotube wires calculated in references[7, 9, 27] is large, implying that nanotubes are good molecular wires. The reflection probability at energies away from the band center (where many sub-bands coexist) is much larger. At energies corresponding to the opening of new sub-bands, coupling of high and low velocity states causes a dip in the transmission, which should be observable in experiments where the Fermi energy can be tuned. The transmission probability through nanotube wires with strong scatterers were also calculated. These structures show a transmission gap around E=0, whose width increases with the number of defects.

Transport experiments have demonstrated that carbon nanotubes are excellent

[a] In addition to the transmission resonance around $0.25eV$, there is a new narrow resonance around $0.5eV$ in Fig. 6. This new resonance is due to quasi-localized states associated with the bond rotation defect. This is discussed further in reference [14].

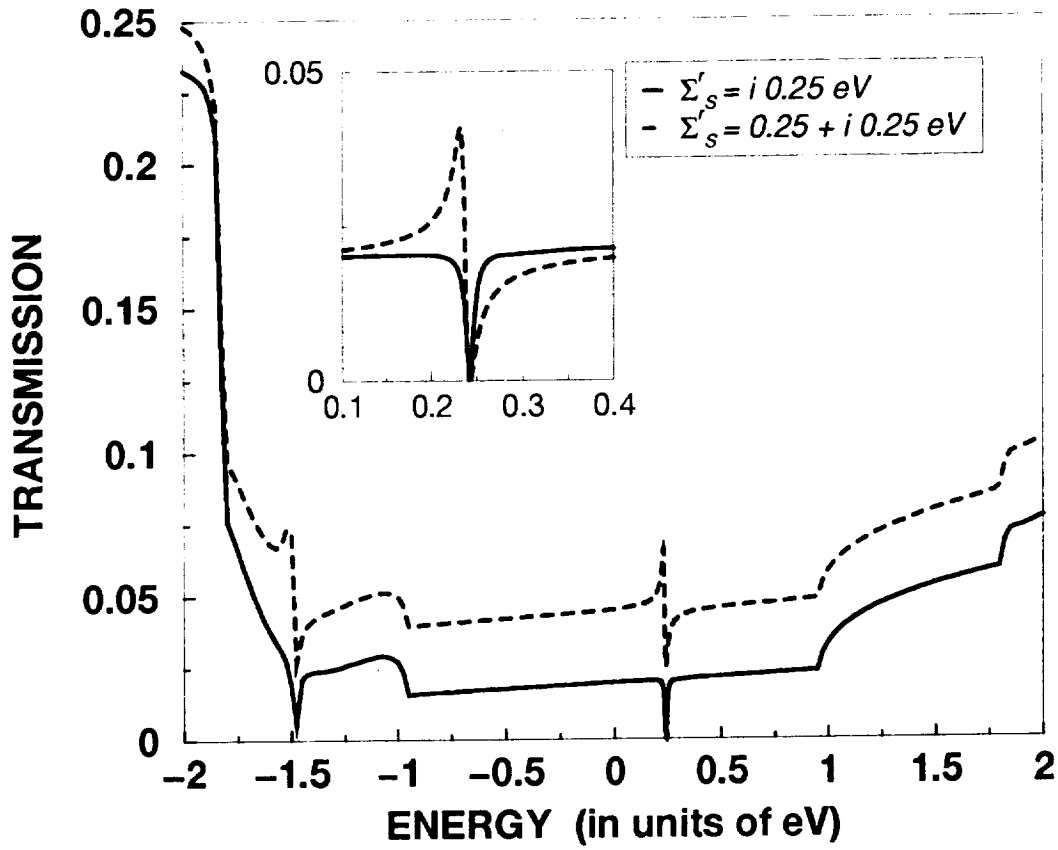

Figure 8: The transmission probability corresponds to the LDOS at most energies except at the peaks in Fig. 7. Around these energies, there is a transmission antiresonance.

metallic molecular wires, having allayed to a large extent the concerns of large contact resistance and the effect of deformation due to coupling with the substrate [5, 6, 28, 29]. While carbon nanotube wires are still far away from real applications in nanoelectronics, they are a good test bed for experiments in both molecular electronics and the basic study of physics in quasi one dimensional systems with electron-electron interactions [29, 30, 31]. These comments would be incomplete without pointing out that references [5] and [6] measure conductances that are very close to integer multiples of $\frac{2e^2}{h}$, instead of integer multiples of $\frac{4e^2}{h}$ that a simple mode counting picture would yield. An open question is if this phenomenon is particular only to these experiments [5, 6] or is it more universal. In any case, a simple and clear explanation of this does not exist at present in the literature.

The second aspect, disussed in section 4 dealt with transport through armchair nanotube wires with polyhedral caps. Localized and continuum energy levels have been shown to coexist [10, 14]. In comparison, asymmetric caps in general lead to quasi-localized states as opposed to localized states, as shown in references [11, 12, 13]. The transmission probabilty from the substrate to an atom in the cap and into the nanotube continuum states follows the LDOS of the atom. The one exception to this is at the energy of the localized states. At this energy, while the LDOS is peaked, the transmission probability exhibits an antiresonance with minimum equal to zero [14]. A defect in the tube causes hybridization between the continuum and localized levels. As a result, scattering due to defects in the tube can transform this sharp antiresonance to a transmission resonance due to new interference paths, similar to the behavior of a structure with two scattering centers. The current carrying capacity of this resonance is however sensitive to the position of the defect in the tube. This makes sense because

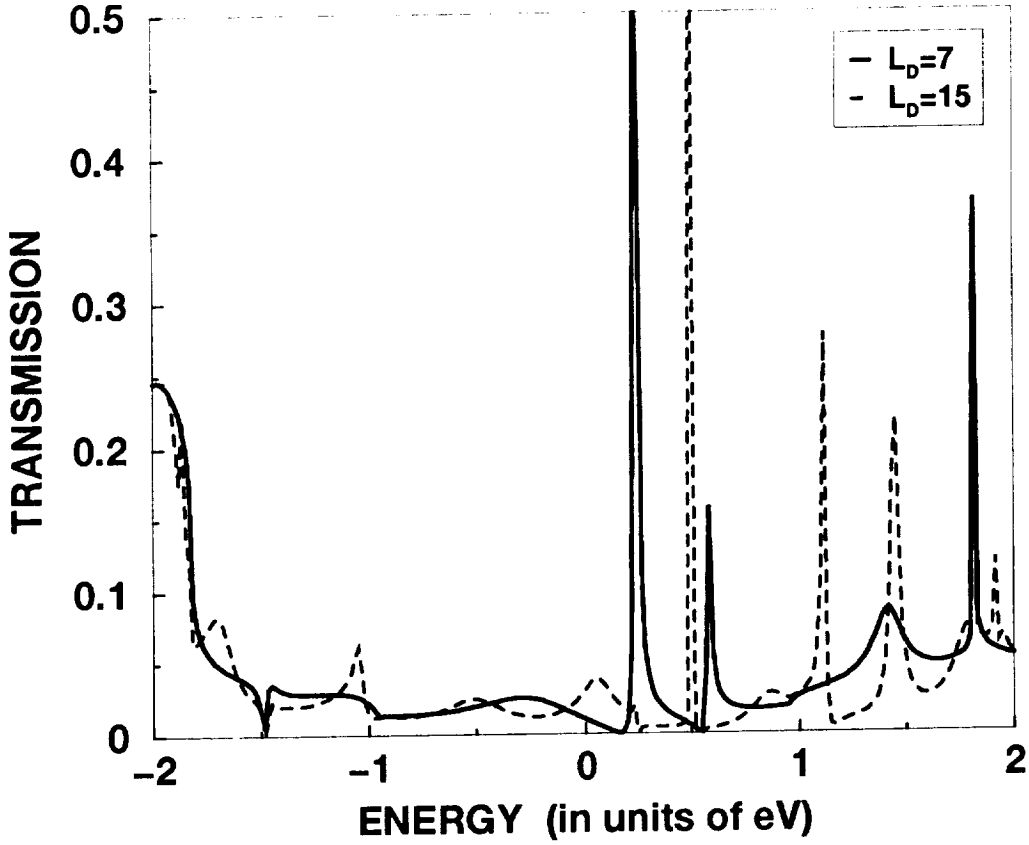

Figure 9: Defects in the nanotube can tranform the sharp antiresonances of Fig. 8 to resonances. The current carrying capacity of the resonance however depends on the location of the defect, as shown by comparing two defect locations.

the hybridization between the continuum and localized levels becomes weaker with an increase in the distance of the defect from the cap.

REFERENCES

1. S. J. Tans, M. Devoret, H. Dai, A. Thess, R.E. Smalley, L.J. Geerligs and C. Dekker, Nature **386**, 474 (1997).
2. P. G. Collins, A. Zettl, H. Bando, A. Thess and R.E. Smalley, Science **278**, 100 (1997).
3. D.H. Cobden, M. Bockrath, N. Chopra, A. Zettl, P.L. McEuen, A. Rinzler, A. Thess, and R.E. Smalley, Physica B **249-251**, 132 (1998).
4. A. Bezryadin, A. R. M. Verschreren, S. J. Tans, and C. Dekker Phys. Rev. Lett. **80**, 4036 (1998).
5. S. Frank, P. Poncharal, Z. L. Wang and W. A. de Heer, Science **280**, 1744 (1998);
6. P. J. de Pablo, E. Graugnard, B. Walsh, R. P. Andres, S. Datta and R. Reifenberger, Appl. Phys. Lett. **74**, 323 (1999)
7. C. T. White and T. N. Todorov Nature , **393**, 240 (1998)
8. T. Ando and T. Nakanishi, J. Phys. Soc. Jpn **67**, 1704 (1998)
9. M. P. Anantram and T. R. Govindan, Phys. Rev. B **58**, 4882 (1998)
10. Ryo Tamura and Masaru Tsukada, Phys. Rev. B **52**, 6015 (1995);
11. D. L. Carroll, P. Redlich, P. M. Ajayan, J. C. Charlier, X. Blase, A. De Vita and R. Car, Phys. Rev. Lett. **78**, 2811 (1997)
12. P. Kim, T. W. Odom, J.-L. Huang and C. M. Lieber, Phys. Rev. Lett. **82**, 1225

(1999)
13. A. De Vita, J.-Ch. Charlier, X. Blase and R. Car, Appl. Phys. A **68**, 283 (1999)
14. M. P. Anantram and T. R. Govindan, *Transmission Through Carbon Nanotubes With Polyhedral Caps*, cond-mat/9907020 (1999)
15. M. P. Anantram, S. Datta and Yongqiang Xue, *Coupling of carbon nanotubes to metallic contacts*, cond-mat/9907357 (1999)
16. C. Caroli, R. Combescot, P. Nozieres and D. Saint-James, J. Phys. C: Solid St. Phys. **4**, 916 (1971).
17. Y. Meir and N.S. Wingreen, Phys. Rev. Lett. **68**, 2512 (1992) discusses the exact regime of validity of this equation.
18. S. Datta, Electronic Transport in Mesoscopic Systems, Cambridge University Press, Cambridge, U.K (1995).
19. W. H. Press, S. A. Teukolsky, W. T. Vetterling and B. P. Flannery, Numerical Recipes in C, The Art of Scientific Computing, Second Edition, Cambridge University Press (1992).
20. M. S. Dresselhaus, G. Dresselhaus and P. C. Eklund, Chap. 19 of Science of Fullerenes and Carbon Nanotubes, Academic Press, New York (1996).
21. C.W.J. Beenakker, Rev. Mod. Phys. **69**, 731 (1997) and references there in.
22. A. Kumar and P. F. Bagwell, Phys. Rev. B **44**, 1747 (1991).
23. L. Chico, V.H. Crespi, L.X. Benedict, S.G. Louie and M.L. Cohen, Phys. Rev. Lett. **76**, 971 (1996).
24. P. F. Bagwell and R. K. Lake, Phys. Rev. B **46**, 15329 (1992); Z. Shao, W. Porod and C. S. Lent, Phys. Rev. B **49**, 7453 (1994); P. Singha Deo and A. M. Jayannavar, Phys. Rev. B **50**, 11629 (1994);
25. U. Fano, Phys. Rev. **124**, 1866 (1961).
26. B. I. Yakobson, App. Phys. Lett. **72**, 918 (1998); M. B. Nardelli et al., Phys. Rev. B **57** 4277 (1998)
27. T. Kortyrko, M. Bartkowiak and G. D. Mahan, Phys. Rev. B **59**, (1999) to appear
28. H. T. Soh, A. F. Morpurgo, J. Kong, C. M. Marcus, C. F. Quate and H. Dai, Preprint (1999).
29. Z. Yao, H. W. Ch. Postma and C. Dekker, Preprint
30. C. Kane, L. Balents, M. P. A. Fisher, Phys. Rev. Lett. **79** 5086 (1997)
31. M. Bockrath, D. H. Cobden, J. Lu, A. G. Rinzler, R. E. Smalley, L. Balents, P. L. Mceuen, *Luttinger Liquid Behavior in Carbon Nanotubes*, cond-mat/9812233